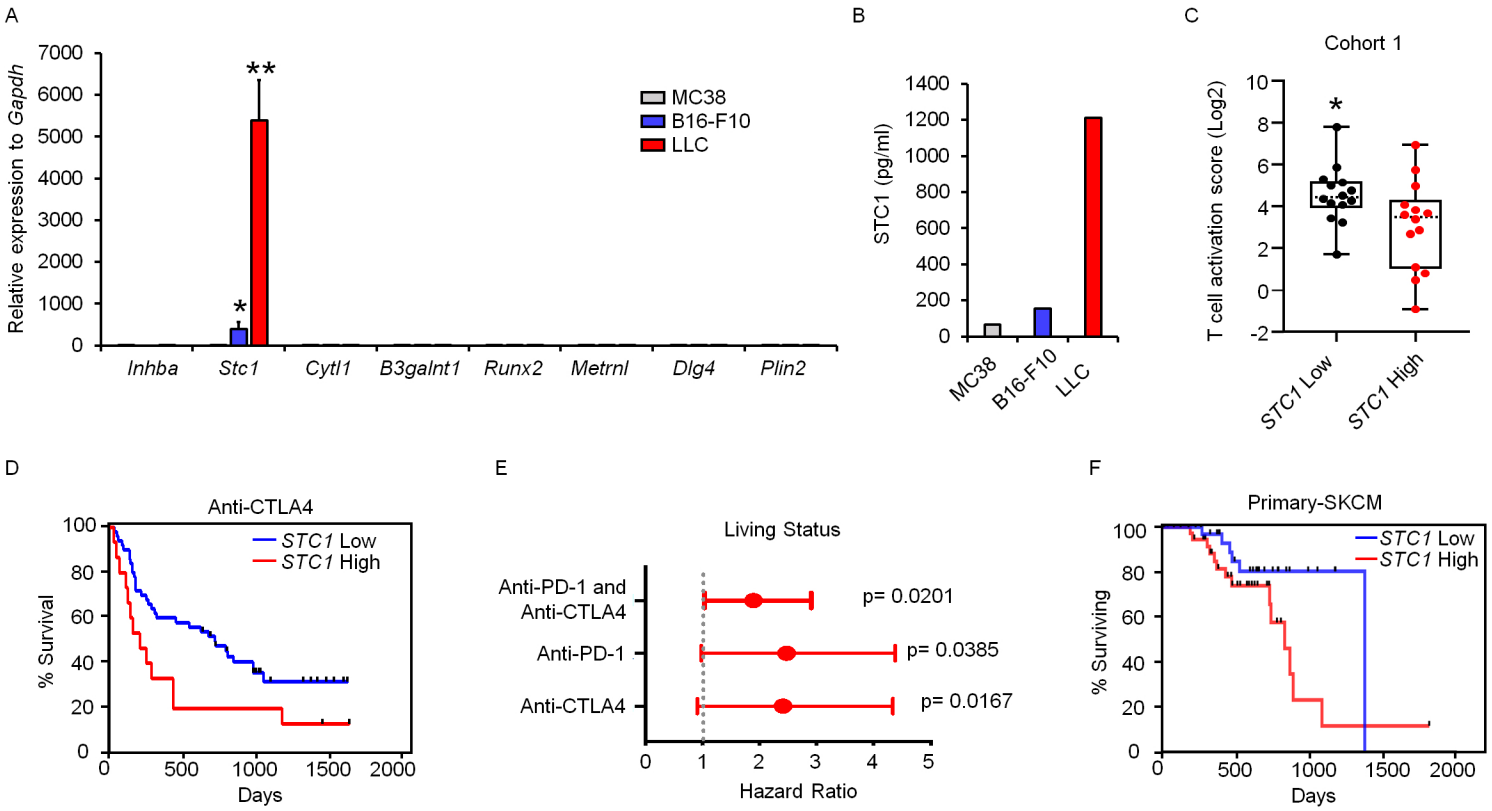

Figure S1, related to Figure 1. *STC1* correlates to cancer resistance to immunotherapy

(A) qPCR showing the top 8 gene transcripts in murine tumor cell lines. Data are presented as mean ± SEM, 2 tail T-test was used for two-way comparisons (n = 3-5, *p < 0.05, **p<0.01).

(B) Murine tumor STC1 released in culture medium measured with ELISA. One of 3 experiments is shown.

(C) Relationship of *STC1* expression with T cell activation in cohort 1. (n = 14, p = 0.031). The dash line represents the median value, the bottom and top of the boxes are the 25th and 75th percentiles (interquartile range). Whiskers encompass 1.5 times the inter-quartile range.

(D) Relationship of *STC1* expression with cancer patient survival. Two combined cohorts treated with anti-CTLA4 (Van-Allen et al., 2015, Nathanson et al., 2017). High (n = 15) and low (n = 50) levels of *STC1* expression, p = 0.0167.

(E) Forest plot representing the adjust value of Cox proportional hazard ratio (HR) in patients treated with anti-PD-1, anti-CTLA4, and the combination as 95% confidential interval (CI) of overall survival.

(F) Relationship of *STC1* expression with cancer patient survival analyzed on primary SKCM. High (n = 38) and low (n = 37) levels of *STC1* expression, p = 0.0387.

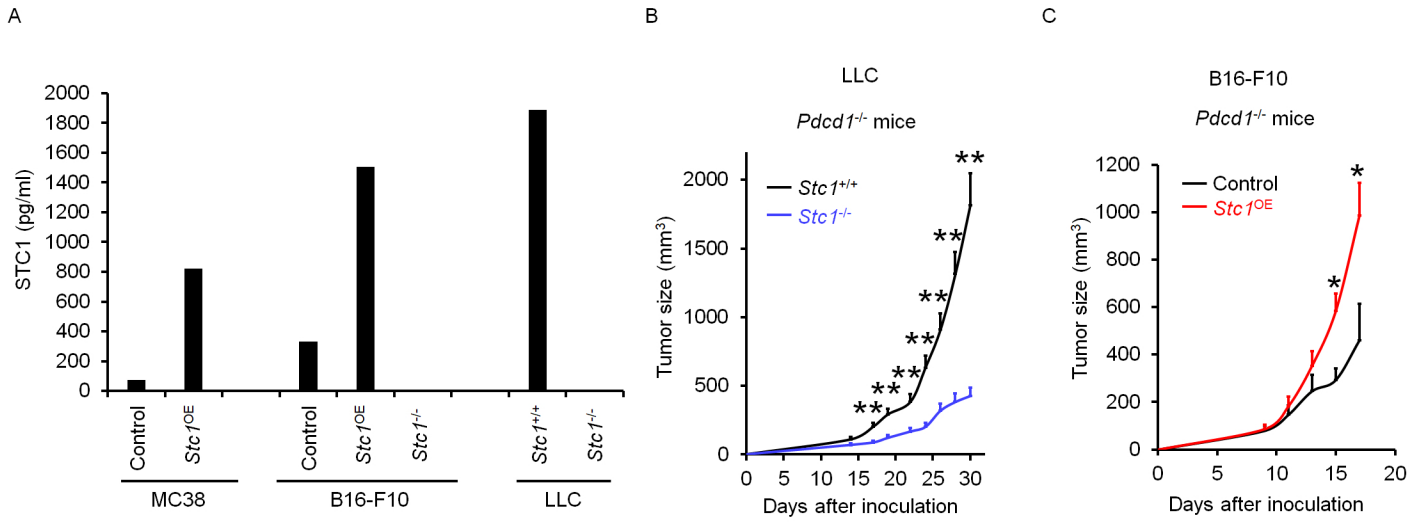

Figure S2, related to Figure 2. Tumor STC1 is critical for intrinsic resistance to tumor immunity

(A) Tumor STC1 released in culture measured with ELISA. One of 3 experiments is shown.

(B-C) Tumor growth curves of *Stc1*$^{+/+}$ and *Stc1*$^{-/-}$ LLC (B) or control and *Stc1*^{OE} B16-F10 (C) in *Pdcd1*$^{-/-}$ C57BL/6J mice. Tumor volume was monitored. Data are shown as mean ± SEM, 2 tail T-test was used for two-way comparisons (n = 5-8, *p < 0.05, **p < 0.01).

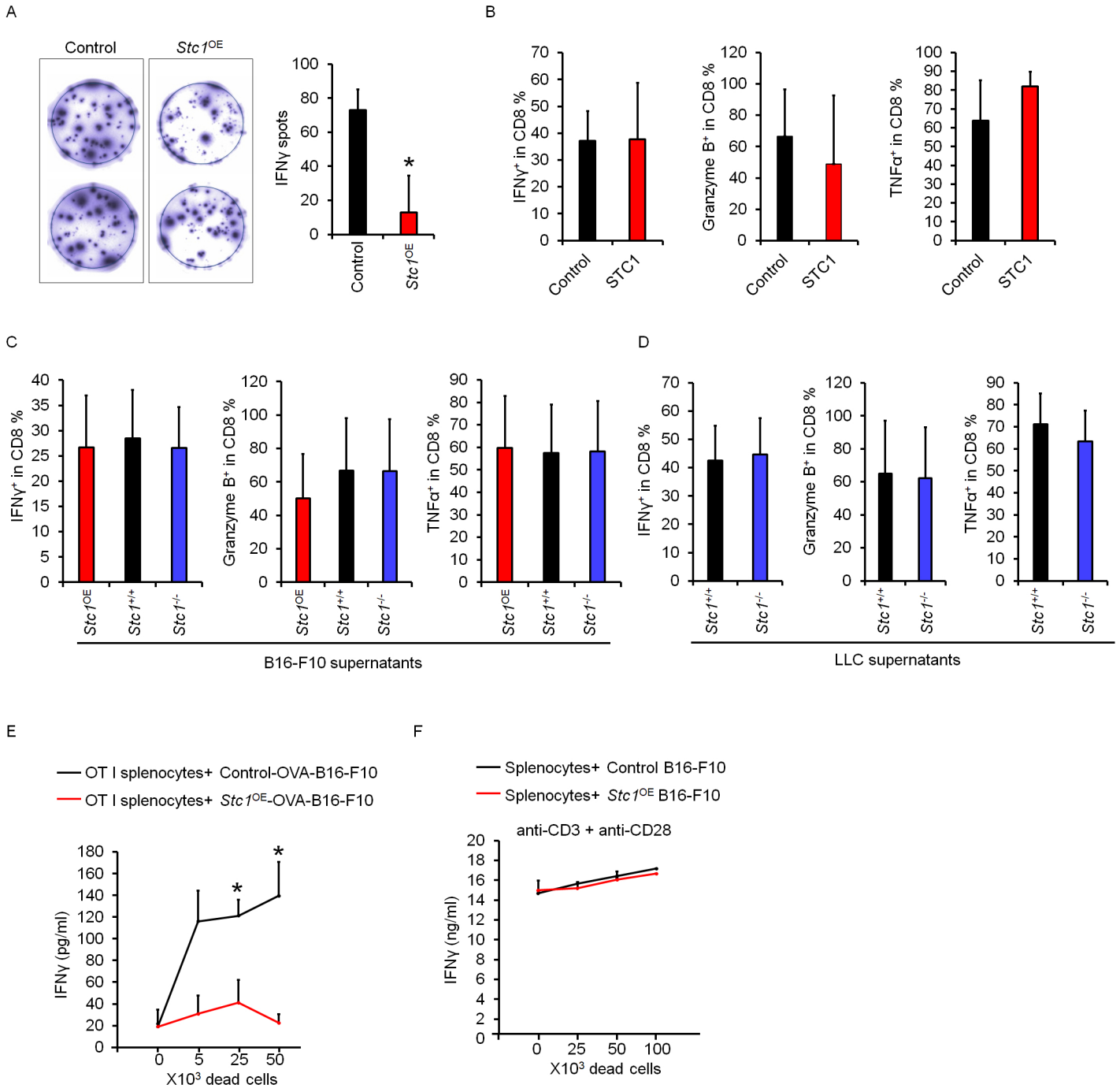

Figure S3, related to Figure 3. Tumor STC1 impairs anti-tumor CD8⁺ T cell responses

(A) IFNγ ELISPOT in tumor drained lymph node T cells from mice bearing control or *Stc1*^{OE} MC38 tumors. Data are shown as mean ± SEM, 2 tail T-test was used for two-way comparisons (n = 5, *p < 0.05).

(B-D) Effect of STC1 on T cell activation. Splenocytes were activated for 72 hours with anti-CD3 and anti-CD28 in the presence of recombinant STC1 (A), or B16-F10 cell culture supernatants (B), or LLC cells culture supernatants (C). FACS showed the percentages of IFNγ⁺, granzyme B⁺, and TNFα⁺CD8⁺ T cells. Data are shown as mean ± SEM, 2 tail T-test was used for two-way comparisons (n = 3, *p < 0.05).

(E) Effect of STC1 on OT-I cell activation. OT-I splenocytes were cultured with dead tumor cells from OVA loaded-B16-F10 cells and OVA loaded- *Stc1*^{OE}-B16-F10 cells for 3 days. ELISA showed IFNγ production. Data are shown as mean ± SEM, 2 tail T-test was used for two-way comparisons (n = 3-4, *p < 0.05).

(F) Effect of STC1 on T cell activation. Splenocytes were activated with anti-CD3 and anti-CD28 for 72 hours in the presence or absence of dead tumor cells from B16-F10 control and *Stc1*^{OE} cells. ELISA showed IFNγ production. Data are shown as mean ± SEM (n = 3-4, *p < 0.05).

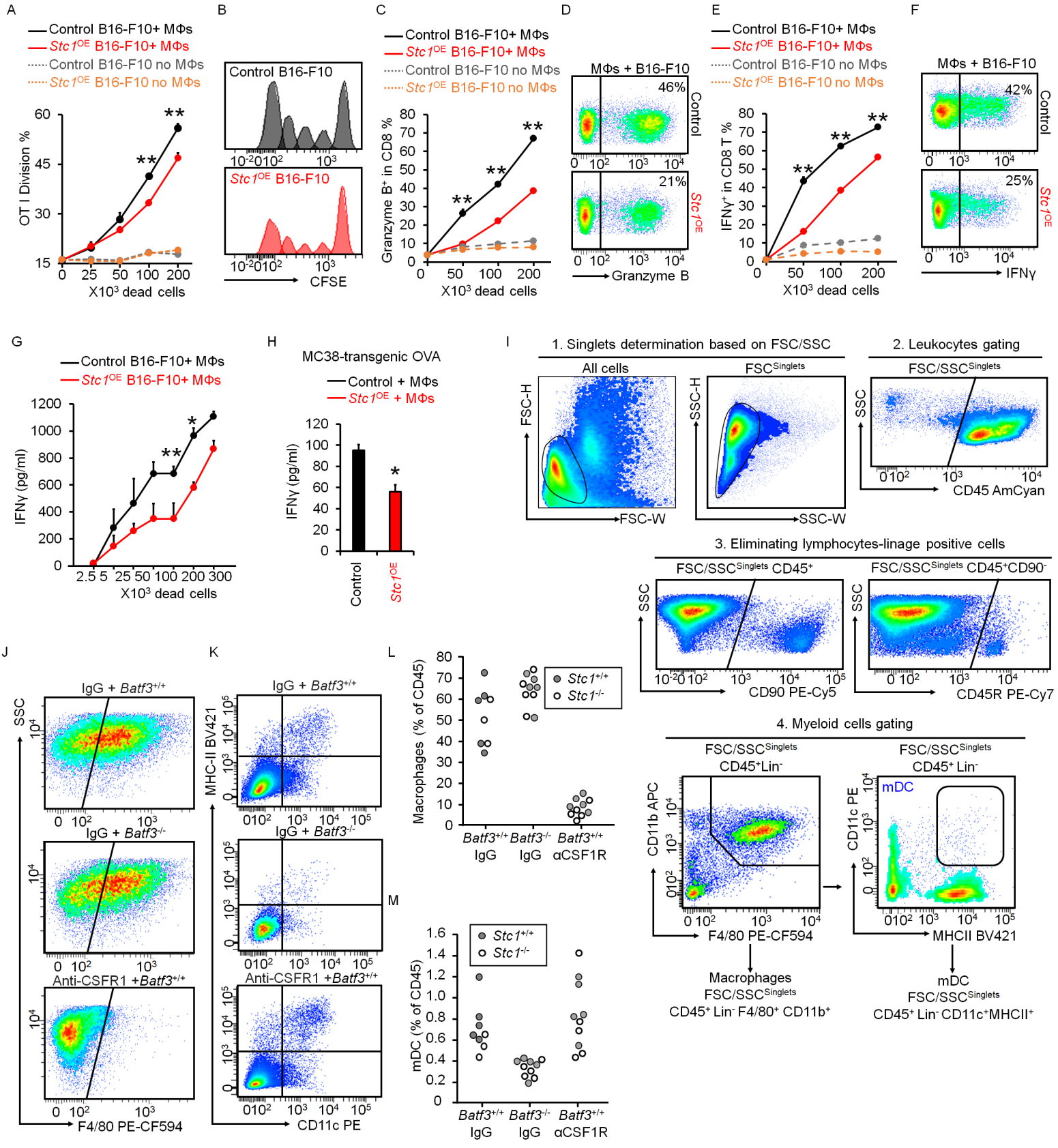
A
Control B16-F10+ MΦs
Stc1OE B16-F10+ MΦs
Control B16-F10 no MΦs
Stc1OE B16-F10 no MΦs
OT I Division %
X10³ dead cells
B
Control B16-F10
Stc1OE B16-F10
CFSE
C
Granzyme B⁺ in CD8 %
X10³ dead cells
D
MΦs + B16-F10
46%
21%
Control
Stc1OE
Granzyme B
E
IFNγ⁺ in CD8 T %
X10³ dead cells
F
MΦs + B16-F10
42%
25%
IFNγ
G
IFNγ (pg/ml)
X10³ dead cells
H
MC38-transgenic OVA
Control + MΦs
Stc1OE + MΦs
IFNγ (pg/ml)
I
1. Singlets determination based on FSC/SSC
All cells
FSC-H
FSC-W
FSCSinglets
SSC-H
SSC-W
2. Leukocytes gating
FSC/SSCSinglets
SSC
CD45 AmCyan
3. Eliminating lymphocytes-linage positive cells
FSC/SSCSinglets CD45+
FSC/SSCSinglets CD45+CD90-
CD90 PE-Cy5
CD45R PE-Cy7
4. Myeloid cells gating
FSC/SSCSinglets CD45+Lin-
CD11b APC
F4/80 PE-CF594
Macrophages
FSC/SSCSinglets
CD45+ Lin- F4/80+ CD11b+
mDC
CD11c PE
MHCII BV421
mDC
FSC/SSCSinglets
CD45+ Lin- CD11c+MHCII+
J
IgG + Batf3+/+
IgG + Batf3-/-
Anti-CSFR1 +Batf3+/+
SSC
F4/80 PE-CF594
K
IgG + Batf3+/+
IgG + Batf3-/-
Anti-CSFR1 +Batf3+/+
MHC-II BV421
CD11c PE
L
Stc1+/+
Stc1-/-
Macrophages (% of CD45)
Batf3+/+ IgG
Batf3-/- IgG
Batf3+/+ αCSF1R
M
Stc1+/+
Stc1-/-
mDC (% of CD45)
Batf3+/+ IgG
Batf3-/- IgG
Batf3+/+ αCSF1R

Figure S4, related to Figure 4. STC1 abrogates tumor immunogenicity via targeting APCs

(A-F) Effect of STC1 on OT-I cell activation. B16-F10 cells and *Stc1*^{OE} B16-F10 cells were loaded with OVA and killed with UV-irradiation. CFSE-labeled OT-I cells were cultured for 3 days with different numbers of dead B16-F10 cells and *Stc1*^{OE} B16-F10 cells in the presence of macrophages. FACS showed CSFE dilution (A-B), granzyme B^{+} (C-D), and IFNγ^{+} (E-F) OT-I cells. Data are presented as mean ± SEM, 2 tail T-test was used for two-way comparisons (n = 4-5, **p* < 0.05, **p < 0.01).

(G) ELISA detected OT-I cell released IFNγ in the setting as (A-F). Data are presented as mean ± SEM, 2 tail T-test was used for two-way comparisons (n = 4-5, **p* < 0.05, **p < 0.01).

(H) ELISA detected OT-I cell released IFNγ. The experimental setting is similar to (A-F), but OVA-loaded B16-F10 cells were replaced with OVA transgenic control or *Stc1*^{OE} MC38 cells. Data are presented as mean ± SEM, 2 tail T-test was used for two-way comparisons (n = 5, **p* < 0.05).

(I) Representative FACS gating strategy to define tumor-infiltrating myeloid subsets from LLC tumors.

(J-M) FACS showing the changes of macrophages and DCs in LLC tumors under the treatment of IgG or anti-CSF1R in WT or *Batf3*$^{-/-}$ mice.

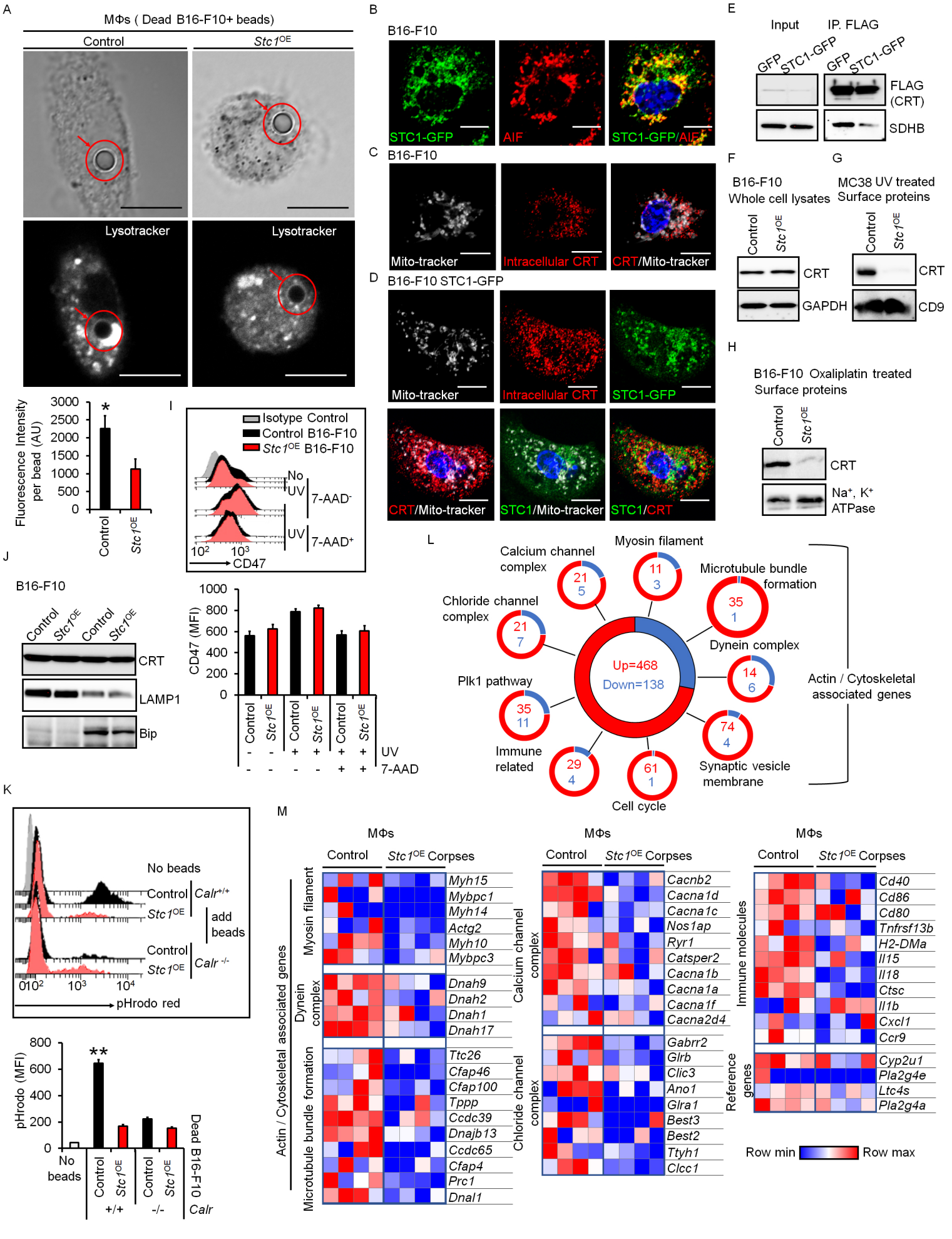
A
MΦs (Dead B16-F10+ beads)
Control
Stc1OE
Lysotracker
Lysotracker
B
B16-F10
STC1-GFP
AIF
STC1-GFP/AIF
C
B16-F10
Mito-tracker
Intracellular CRT
CRT/Mito-tracker
D
B16-F10 STC1-GFP
Mito-tracker
Intracellular CRT
STC1-GFP
CRT/Mito-tracker
STC1/Mito-tracker
STC1/CRT
E
Input
IP. FLAG
GFP
STC1-GFP
GFP
STC1-GFP
FLAG (CRT)
SDHB
F
B16-F10 Whole cell lysates
Control
Stc1OE
CRT
GAPDH
G
MC38 UV treated Surface proteins
Control
Stc1OE
CRT
CD9
H
B16-F10 Oxaliplatin treated Surface proteins
Control
Stc1OE
CRT
Na+, K+ ATPase
Fluorescence Intensity per bead (AU)
3000
2500
2000
1500
1000
500
0
*
Control
Stc1OE
I
Isotype Control
Control B16-F10
Stc1OE B16-F10
No UV
UV
7-AAD-
7-AAD+
10^2
10^3
CD47
J
B16-F10
Control
Stc1OE
Control
Stc1OE
CRT
LAMP1
Bip
CD47 (MFI)
1000
800
600
400
200
0
Control
Stc1OE
Control
Stc1OE
Control
Stc1OE
UV
7-AAD
L
Myosin filament
11
3
Calcium channel complex
21
5
Microtubule bundle formation
35
1
Chloride channel complex
21
7
Dynein complex
14
6
Up=468
Down=138
Plk1 pathway
35
11
Actin / Cytoskeletal associated genes
Immune related
29
4
61
1
74
4
Synaptic vesicle membrane
Cell cycle
K
No beads
Control
Calr+/+
Stc1OE
add beads
Control
Calr -/-
Stc1OE
010^2
10^3
10^4
pHrodo red
pHrodo (MFI)
800
600
400
200
0
**
No beads
Control
Stc1OE
Control
Stc1OE
+/+
-/-
Dead B16-F10 Calr
M
MΦs
Control
Stc1OE Corpses
Actin / Cytoskeletal associated genes
Myosin filament
Myh15
Mybpc1
Myh14
Actg2
Myh10
Mybpc3
Dynein complex
Dnah9
Dnah2
Dnah1
Dnah17
Microtubule bundle formation
Ttc26
Cfap46
Cfap100
Tppp
Ccdc39
Dnajb13
Ccdc65
Cfap4
Prc1
Dnal1
Calcium channel complex
Cacnb2
Cacna1d
Cacna1c
Nos1ap
Ryr1
Catsper2
Cacna1b
Cacna1a
Cacna1f
Cacna2d4
Chloride channel complex
Gabrr2
Glrb
Clic3
Ano1
Glra1
Best3
Best2
Ttyh1
Clcc1
Immune molecules
Cd40
Cd86
Cd80
Tnfrsf13b
H2-DMa
Il15
Il18
Ctsc
Il1b
Cxcl1
Ccr9
Reference genes
Cyp2u1
Pla2g4e
Ltc4s
Pla2g4a
Row min
Row max

Figure S5, related to Figure 5. Tumor STC1 traps CRT to inhibit macrophage function

(A) Effect of STC1 on macrophage-mediated bead up-take. Macrophages were incubated with dead cells from B16-F10 cells and *Stc1*^{OE} B16-F10 cells. Latex beads were added (arrow). Macrophages were stained with lysotracker dye (white). Scale bars: 10 μm. Results are shown as the fluorescence intensity of lysotracker dye at the bead areas in macrophage phagosomes, mean ± SEM (n = 6, **p < 0.05).

(B) Localization of STC1. UV-treated STC1-GFP expressing B16-F10 cells were stained for GFP (STC1-GFP) (Green), AIF (red), and DAPI (blue). Confocal images showed the co-localization of STC1 and AIF. Scale bars: 10 μm. One of 3 experiments is shown.

(C) Localization of CRT. UV-treated B16-F10 cells were stained for mito-tracker (white), CRT (Red) and DAPI (blue). Confocal images showed the co-localization of mito-tracker and CRT. Scale bars: 10 μm. One of 3 is shown.

(D) Co-localization of STC1 and CRT. UV-treated STC1-GFP expressing B16-F10 cells were stained for mito-tracker (white), CRT(Red), GFP (STC1-GFP) (Green), and DAPI (blue). Confocal images showed the co-localization of mito-tracker, CRT, and STC1 (STC1-GFP) (Green). Scale bars: 10 μm. One of 3 experiments is shown.

(E) Co-IPs of CRT-FLAG with SDHB were performed in cell lysates from UV-treated B16-F10 cells. One of 2 experiments is shown.

(F) Western blots showing expression of CRT in whole cell lysates from UV-treated B16-F10 cells and *Stc1*^{OE} B16-F10 cells. One of 2 experiments is shown.

(G) MC38 cell membrane CRT. Surface proteins from UV-treated or un-treated MC38 vehicle control cells and *Stc1*^{OE} cells were labeled with biotin. Western blots showed cell membrane CRT and CD9 in biotin-labeled proteins. CD9 serves as membrane protein control. One of 2 experiments is shown.

(H) B16-F10 cell membrane CRT. Surface proteins from oxaliplatin treated B16-F10 control cells and *Stc1*^{OE} cells were labeled with biotin. Western blots showed cell membrane CRT and Na^+, K^+ ATPase α1 in biotin-labeled proteins. Na^+, K^+ ATPase α1 serves as membrane protein control. One of 2 experiments is shown.

(I) FACS showing mean fluorescence intensity (MFI) of CD47 on UV-treated or un-treated B16-F10 control cells and *Stc1*^{OE} cells. Gated on either 7-AAD$^-$ or 7-AAD$^+$. Data are shown as mean ± SEM (n = 4).

(J) Western blots showing distribution of CRT in lysosome (LAMP1) and ER (Bip) from UV-treated B16-F10 cells and *Stc1*^{OE} B16-F10 cells. One of 2 experiments is shown.

(K) Macrophage-mediated bead up-take. Macrophages were incubated with dead cells from *Calr* $^{+/+}$ or *Calr* $^{-/-}$ B16-F10 and *Stc1*^{OE} B16-F10 cells for 20 hours. pHrodo™-SE labeled 3 μm latex beads were added for an additional 1 hour. FACS showed mean red fluorescence intensity (MFI) in macrophages. Gated on $CD11b^+CD45^+$. Data are shown as mean ± SEM (n = 4, **p<0.01).

(L-M) RNA-seq of macrophages engulfed control B16-F10 tumors and *Stc1*^{OE} B16-F10 tumors. Gene signatures were normalized to macrophages without engulfment. The heatmap depicts representative gene clusters differentially expressed between macrophages engulfed control B16-F10 tumors and *Stc1*^{OE} B16-F10 tumors.

Table S1, related to Figure 5. Mass spectrometry analysis of proteins interacting with STC1

Identified Proteins	Accession Number	Total Spectrum Count		Ratio ($STC1^{FLAG}$/ Control)
		Control	$STC1^{FLAG}$	
Stanniocalcin-1	sp|O55183|STC1_MOUSE	0	71	N/A
Protein disulfide-isomerase A3	sp|P27773|PDIA3_MOUSE	0	31	N/A
Metastasis-associated protein MTA2	sp|Q9R190|MTA2_MOUSE	0	26	N/A
Calreticulin	sp|P14211|CALR (CRT)_MOUSE	0	19	N/A
Transforming acidic coiled-coil-containing protein 1	sp|Q6Y685|TACC1_MOUSE	0	17	N/A
Heat shock protein HSP 90-alpha	sp|P07901|HS90A_MOUSE	0	10	N/A
Elongation factor 1-alpha 1	sp|P10126|EF1A1_MOUSE	0	9	N/A
Intracellular hyaluronan-binding protein 4	tr|E9QKB2|E9QKB2_MOUSE	0	9	N/A
Isoform 2 of 14-3-3 protein theta	sp|P68254-2|1433T_MOUSE	0	8	N/A
U5 small nuclear ribonucleoprotein 200 kDa helicase	sp|Q6P4T2|U520_MOUSE	0	7	N/A
14-3-3 protein eta	sp|P68510|1433F_MOUSE	0	7	N/A
Tight junction protein ZO-1	sp|P39447|ZO1_MOUSE	0	6	N/A
Methyl-CpG-binding domain protein 2	sp|Q9Z2E1|MBD2_MOUSE	0	6	N/A
Protein disulfide-isomerase A6	tr|Q3TML0|Q3TML0_MOUSE	0	6	N/A
Pre-mRNA-processing-splicing factor 8	sp|Q99PV0|PRP8_MOUSE	0	5	N/A
Polyadenylate-binding protein 1	sp|P29341|PABP1_MOUSE	0	5	N/A
26S protease regulatory subunit 7	tr|Q8BVQ9|Q8BVQ9_MOUSE	0	5	N/A
Nucleophosmin	sp|Q61937|NPM_MOUSE	0	5	N/A
Protein RCC2	sp|Q8BK67|RCC2_MOUSE	0	5	N/A
Tubulin beta-5 chain	sp|P99024|TBB5_MOUSE	0	5	N/A
Eukaryotic translation initiation factor 3 subunit C	sp|Q8R1B4|EIF3C_MOUSE	0	5	N/A
Isoform 2 of F-actin-capping protein subunit beta	sp|P47757-2|CAPZB_MOUSE	0	5	N/A
Dynactin subunit 2	sp|Q99KJ8|DCTN2_MOUSE	0	5	N/A
Chromobox protein homolog 3	sp|P23198|CBX3_MOUSE	0	5	N/A
Endoplasmin	sp|P08113|ENPL_MOUSE	0	5	N/A
Chromodomain-helicase-DNA-binding protein 4	sp|Q6PDQ2|CHD4_MOUSE	0	4	N/A
Aminoacyl tRNA synthase complex-interacting multifunctional protein 1	sp|P31230|AIMP1_MOUSE	0	4	N/A
Cyclin-dependent kinase 2-associated protein 1	sp|O35207|CDKA1_MOUSE	0	4	N/A
Single-stranded DNA-binding protein	tr|Q8R2K3|Q8R2K3_MOUSE	0	4	N/A
TBC1 domain family member 5	sp|Q80XQ2|TBCD5_MOUSE	0	4	N/A
Pre-mRNA-splicing factor RBM22	sp|Q8BHS3|RBM22_MOUSE	0	4	N/A
10 kDa heat shock protein, mitochondrial	sp|Q64433|CH10_MOUSE	0	4	N/A
Src substrate cortactin	sp|Q60598|SRC8_MOUSE	0	4	N/A
Peroxiredoxin-2	sp|Q61171|PRDX2_MOUSE	0	4	N/A
40S ribosomal protein S19	sp|Q9CZX8|RS19_MOUSE	0	4	N/A
60S acidic ribosomal protein P0	sp|P14869|RLA0_MOUSE	0	4	N/A
Elongation factor 2	sp|P58252|EF2_MOUSE	0	4	N/A
Protein TSSC4	sp|Q9JHE7|TSSC4_MOUSE	0	4	N/A
Tubulin beta-4B chain	sp|P68372|TBB4B_MOUSE	0	4	N/A
Isoleucine--tRNA ligase, cytoplasmic	sp|Q8BU30|SYIC_MOUSE	0	3	N/A
Protein Qars	tr|D3Z158|D3Z158_MOUSE	0	3	N/A
KN motif and ankyrin repeat domain-containing protein 4	sp|Q6P9J5|KANK4_MOUSE	0	3	N/A
Stromal cell-derived factor 2	tr|A0A0R4IZW9|A0A0R4IZW9_MOUSE	0	3	N/A
Alpha-centractin	sp|P61164|ACTZ_MOUSE	0	3	N/A
Elongation factor 1-gamma	sp|Q9D8N0|EF1G_MOUSE	0	3	N/A
oxoglutarate dehydrogenase complex, mitochondrial	sp|Q9D2G2|ODO2_MOUSE	0	3	N/A
U2 small nuclear ribonucleoprotein A	sp|P57784|RU2A_MOUSE	0	3	N/A
Protein disulfide-isomerase	sp|P09103|PDIA1_MOUSE	0	3	N/A
Eukaryotic translation initiation factor 3 subunit G	sp|Q9Z1D1|EIF3G_MOUSE	0	3	N/A
PERQ amino acid-rich with GYF domain-containing protein 2	sp|Q6Y7W8|PERQ2_MOUSE	0	3	N/A
Eukaryotic translation initiation factor 3 subunit K	sp|Q9DBZ5|EIF3K_MOUSE	0	3	N/A
60S ribosomal protein L12	sp|P35979|RL12_MOUSE	0	3	N/A
Isoform 2 of Polycomb protein EED	sp|Q921E6-2|EED_MOUSE	0	3	N/A

Data can be found at ProteomeXchange consortium: PXD023251

40S ribosomal protein SA	sp|P14206|RSSA_MOUSE	0	3	N/A
Reticulocalbin-2	sp|Q8BP92|RCN2_MOUSE	0	3	N/A
Nucleolar RNA helicase 2	sp|Q9JIK5|DDX21_MOUSE	0	3	N/A
Complement component 1 Q subcomponent-binding protein	tr|Q8R5L1|Q8R5L1_MOUSE	0	3	N/A
Small nuclear ribonucleoprotein Sm D1	sp|P62315|SMD1_MOUSE	0	3	N/A
26S protease regulatory subunit 6B	sp|P54775|PRS6B_MOUSE	0	3	N/A
40S ribosomal protein S20	sp|P60867|RS20_MOUSE	0	3	N/A
Eukaryotic translation initiation factor 3 subunit M	sp|Q99JX4|EIF3M_MOUSE	0	3	N/A
Endoplasmic reticulum resident protein 29	sp|P57759|ERP29_MOUSE	0	3	N/A
Vesicle-associated membrane protein-associated protein B	sp|Q9QY76|VAPB_MOUSE	0	3	N/A
26S proteasome non-ATPase regulatory subunit 11	sp|Q8BG32|PSD11_MOUSE	0	3	N/A
Isoform 2 of Poly(U)-binding-splicing factor PUF60	sp|Q3UEB3-2|PUF60_MOUSE	0	3	N/A
Aspartate--tRNA ligase, cytoplasmic	sp|Q922B2|SYDC_MOUSE	0	3	N/A
Isoform 2 of Peptidyl-prolyl cis-trans isomerase H	sp|Q9D868-2|PPIH_MOUSE	0	3	N/A
Polyadenylate-binding protein 2	sp|Q8CCS6|PABP2_MOUSE	0	2	N/A
LanC-like protein 1	sp|O89112|LANC1_MOUSE	0	2	N/A
Collagen alpha-5(VI) chain	sp|A6H584|CO6A5_MOUSE	0	2	N/A
Probable cytosolic iron-sulfur protein assembly protein CIAO1	sp|Q99KN2|CIAO1_MOUSE	0	2	N/A
Eukaryotic translation initiation factor 4B	sp|Q8BGD9|IF4B_MOUSE	0	2	N/A
U1 small nuclear ribonucleoprotein A (Fragment)	tr|D3Z0S6|D3Z0S6_MOUSE	0	2	N/A
Dehydrogenase/reductase SDR family member 4	sp|Q99LB2|DHRS4_MOUSE	0	2	N/A
Ferritin light chain 1	sp|P29391|FRIL1_MOUSE	0	2	N/A
Coatomer subunit beta	sp|O55029|COPB2_MOUSE	0	2	N/A
CD2 antigen cytoplasmic tail-binding protein 2	sp|Q9CWK3|CD2B2_MOUSE	0	2	N/A
Leucine--tRNA ligase, cytoplasmic	sp|Q8BMJ2|SYLC_MOUSE	0	2	N/A
mitochondrial	sp|Q9CQA3|SDHB_MOUSE	2	17	8.5
Rho guanine nucleotide exchange factor (GEF7), isoform CRA_a	tr|A0A0R4J0X8|A0A0R4J0X8_MOUSE	4	23	5.8
(Bos taurus) similar to alpha-tubulin I isoform 1	ENSEMBL:ENSBTAP00000016242	2	9	4.5
Isoform 2 of Cellular nucleic acid-binding protein	sp|P53996-2|CNBP_MOUSE	3	12	4.0
Stromal cell-derived factor 2-like protein 1	sp|Q9ESP1|SDF2L_MOUSE	3	11	3.7
Transcriptional repressor p66-beta	sp|Q8VHR5|P66B_MOUSE	14	46	3.3
Isoform 2 of Methyl-CpG-binding domain protein 3	sp|Q9Z2D8-2|MBD3_MOUSE	5	16	3.2
Metastasis-associated protein MTA1	sp|Q8K4B0|MTA1_MOUSE	15	44	2.9
Transcriptional repressor p66 alpha	sp|Q8CHY6|P66A_MOUSE	13	38	2.9
Splicing factor 3B subunit 3	sp|Q921M3|SF3B3_MOUSE	5	14	2.8
Bifunctional glutamate/proline--tRNA ligase	sp|Q8CGC7|SYEP_MOUSE	6	16	2.7
Lysine--tRNA ligase	sp|Q99MN1|SYK_MOUSE	9	24	2.7
Elongation factor 1-delta	sp|P57776|EF1D_MOUSE	2	5	2.5
Elongation factor 1-beta	sp|O70251|EF1B_MOUSE	4	10	2.5
116 kDa U5 small nuclear ribonucleoprotein component	sp|O08810|U5S1_MOUSE	4	10	2.5
Transmembrane glycoprotein NMB	sp|Q99P91|GPNMB_MOUSE	6	15	2.5
Isoform 3 of Transforming acidic coiled-coil-containing protein 2	sp|Q9JJG0-3|TACC2_MOUSE	43	105	2.4
cAMP-dependent protein kinase type I-alpha regulatory subunit	sp|Q9DBC7|KAP0_MOUSE	5	12	2.4
Peroxiredoxin-1	sp|P35700|PRDX1_MOUSE	3	7	2.3
Isoform HSP105-beta of Heat shock protein 105 kDa	sp|Q61699-2|HS105_MOUSE	4	9	2.3

Data can be found at ProteomeXchange consortium: PXD023251